# THE EFFECT OF WIPER EDGE INSERTS ON THE SPECIFIC CUTTING ENERGY IN FACE MILLING OF ALUMINIUM ALLOYS

**António Mourão[1], Laurențiu Slătineanu[2] & António M. Gonçalves-Coelho[1]**

[1] UNIDEMI, Universidade Nova de Lisboa, Faculdade de Ciências e Tecnologia, 2829-516 Caparica, Portugal
[2] "Gheorghe Asachi" Technical University of Iasi, Blvd. Mangeron No. 59A, 700050 Iasi, Romania

Corresponding author: António M. Gonçalves-Coelho, goncalves.coelho@fct.unl.pt

***Abstract:*** Wiper edge tool inserts are used to improve the surface finishing in milling, so that a final grinding is avoided. Wiper edge inserts can also be used in rough cutting for improving productivity without compromising the final surface quality. Accurate estimations of cutting force and power are important for productivity, since they help choosing the right machine, tools and fixtures. Those estimations depend on the specific cutting energy, which in turn depends on the hardness of the machined material, the cutting parameters, and the geometry of the tool. The common computation of specific cutting energy just considers the feed per tooth or the unformed chip thickness, but the insert shape should also be considered. This paper shows that the specific cutting energy in face milling with zero nose radius wiper edge inserts is similarly influenced by the depth of cut and by the feed per tooth. Additionally, cutting speed should not be neglected.

***Keywords:*** Specific cutting energy, face milling, aluminium alloys, wiper edge inserts, productivity.

## 1. INTRODUCTION

Wiper edge technology for tool inserts has been used for years as a means to improve the surface finishing in milling operations, in such a manner that a final grinding operation can often be avoided. In fact, this technology allows attaining values of the mean roughness ($R_a$) below 0,4 μm in face milling of aluminium alloys. Beside to finishing, wiper edge inserts are being used regularly for rough cutting with increasing productivity without compromising the final surface quality, as claimed by some of the most important tools manufacturers (Kennametal 2010; Mitsubishi 2010) and supported by some studies (Mourão 1999). The same manufacturers also claim that wiper edge technology prevents the occurrence of chatter to some extent. Therefore, it seems that it is feasible to increase the productivity of the cutting processes by using higher feed rates and/or cutting depths, while keeping, or even improving, the final quality of the machined surfaces. This is why nowadays there is a trend for using this kind of inserts in operations with higher cutting energy.

Yet, the changes in the geometry of the wiper edges cause significant variations of the specific cutting energy (Rodrigues & Coelho, 2007), a circunstance that should be taken into account when choosing the most efficient machine tools and work piece fixtures.
Broadly speaking, the accurate estimation of the cutting forces is important for planning and setting up high productivity machining process.
However, the aforesaid estimation critically depends on the prediction of the specific cutting energy, which in turn depends on the hardness of the material to be machined, on the cutting parameters, and on the geometry of the tool and inserts.
In addition, the practical formulae currently used for computing the specific cutting energy in milling operations only take into account the feed per tooth or the thickness of the unformed chip, as for example

$$k_s = k_r \left( \frac{0,2}{h_m} \right)^{0,29} , \quad (1)$$

where $k_s$ is the actual specific cutting energy, $k_r$ is the specific cutting energy for a reference feed per revolution, and $h_m$ is the mean thickness of the undeformed chip (Sandvik-Coromant 1994). However, such formulae, do not take into account the variety of insert shapes that are being used nowadays.
The present work is a contribution for lessening the lack of information on these kind of processes, which shows that the specific cutting energy in face milling of aluminium alloys with zero nose radius wiper edge inserts is similarly influenced by both the depth of cut and the feed per tooth. Additionally, it shows that the cutting speed should not be neglected.
The motivation of the authors for writing this paper was even increased because, as far as they know, there is no published data about the specific cutting energy of aluminium alloy work pieces in milling operations with zero nose radius wiper edge inserts, and the major makers of milling tools recommend this kind of inserts for the purpose.

## 2. THE EXPERIMENTAL PROCEDURE

### 2.1 The methodology

A Design of Experiments (DoE) technique was adopted to process the experimental data aquired through face milling of aluminium alloy work pieces. The studied response was the cutting force, as required for computing the specific cutting energy through the equation

$$k_s = \frac{F_c}{a_p f_z}, \quad (2)$$

where $k_s$ is the specific cutting energy, $F_c$ the cutting force, $a_p$ the depth of cut, and $f_z$ the feed per tooth.

Four variables were considered for building our experimental model, three of them associated with the control of the milling process (the cutting speed, $v$; the feed per tooth, $f_z$; and the depth of cut, $a_p$) and one related to characteristics of the material to be machined (the material hardness, HB).

A central composite design (CCD) was used to find a model that represents the effects of the variables and of their interactions through a second-degree polynomial function (Montgomery, 1991):

$$Y = \beta_0 + \sum_{i=1}^{k} \beta_i X_i + \sum_{i=1}^{k} \beta_{ii} X_i^2 + \sum_{i=1}^{k-1} \sum_{j>i}^{k} \beta_{ij} X_i X_j + \varepsilon, \quad (3)$$

where $Y$ is the modeled response, $X_i$ are the variables, $\beta_0$, $\beta_i$, $\beta_{ii}$ and $\beta_{ij}$ are the regression coefficients of the parameters and $\varepsilon$ is the experimental error.

The most important characteristic of the polynomial models is their ability for representing non-monotonic responses with a high accuracy over a large range of their variables. This makes these models very useful when studying phenomena for which the monotonic response hypothesis is not plausible.

The second-degree polynomial model for $k_s$ is obtained by substituting in Eq. (2) the response model that represents $F_c$, which in turn is a function of the form of Eq. (3). According to the plan of experiments that was used to obtain the model of Eq. (3), all the variables should assume five different values that correspond to the coded values -2, -1, 0, 1, 2. Table 1 contains the levels that were used for the coded variables ($x_i$) and the corresponding values for the actual variables ($X_i$).

Table 1. The plan of experiments

| Levels of the Coded Variables ($x_i$) | | | -2 | -1 | 0 | 1 | 2 |
|---|---|---|---|---|---|---|---|
| Variables ($X_i$) | $v$ (m/min) | | 600 | 700 | 814 | 947 | 1100 |
| | $f_z$ (mm) | | 0,07 | 0,10 | 0,14 | 0,20 | 0,28 |
| | $a_p$ (mm) | | 0,30 | 0,60 | 1,17 | 2,30 | 4,50 |
| | Hardness (HB) | Theoretical | 80 | 98 | 120 | 148 | 182 |
| | | Practical | 70 | 98 | 120 | 148 | 167 |

The actual values of Table 1 were selected according to a rotatable central composite design (CCD) with realistic ranges for all the variables, given the characteristics of the machining centre and of the current wide range of machinable aluminium alloys. However, in practical terms, the theoretical values for the Brinell hardness could not be used.

The coded levels -1 and +1 for the variables of the same Table were selected as representative of low and high values, respectively, taking into account typical values that can be found both in the literature and in the real-world practice. For the remaining levels, the corresponding values were computed through

$$X_i = \exp\left(x_i \ln X_R + \ln X_M\right) \quad (4)$$

where $X_i$ is the value of the variable for the level $x_i$ and $X_m$ and $X_R$ are computed through Eq. (5) and Eq. (6), respectively.

$$X_m = \exp\frac{\left(\ln X_{+1} + \ln X_{-1}\right)}{2} \quad (5)$$

$$X_R = \exp\frac{\left(\ln X_{+1} - \ln X_{-1}\right)}{2} \quad (6)$$

The values labelled as “Practical” in Table 1 correspond to the commercially available aluminium alloys with the closest values to the theoretically required hardness, as shown in Table 2, where one can see that the values for the hardness announced by the makers of the alloys (the “expected” values) were confirmed by us experimentally (the “actual” values).

Table 2. Hardness of the used aluminium alloys

| Alloy type | Composition (DIN 1712) | Brinell Hardness (expected) | Brinell Hardness (effective) |
|---|---|---|---|
| 5083-HIII | Al Mg 4,5 Mn | 68-75 | 70 |
| 6082-T6 | Al Mg Si 1 | 95 | 98 |
| 2017 A | Al Cu Mg 1 | 105-115 | 120 |
| 7022 T6 | Al Zn Mg Cu 0,5 | 130-150 | 148 |
| 7050 T6 | Al Zn 5,5 Mg Cu | 165-179 | 167 |

This approach compromises the accuracy of the model to some extent, but it is usually adopted in this kind of circumstances (Jain & Bandyopadhyay, 1986; Khabeery & Fattouh, 1986).

### 2.2 The experimental outfit

A Hermle UWF 1202H CNC machining centre (see Fig.1) was used (11,5 kW, 4200 r.p.m. maximum spindle speed).

The machine centre was purposely fitted with a four teeth, 83,6 mm diameter Sandvik-Coromant face milling cutter body type R265.2-80E-20AL, with ISO 1832-1985 SFAN 1203 EFR zero nose radius wiper edge inserts made of uncoated ISO 513-1975 K10 ceramic material, as shown in Fig. 2.

Fig. 1. The Hermle UWF 1202H CNC machining centre

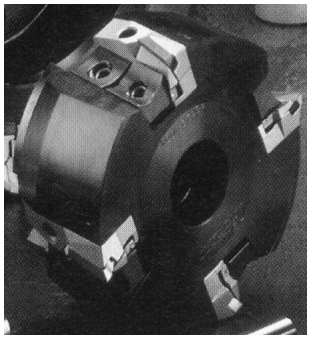

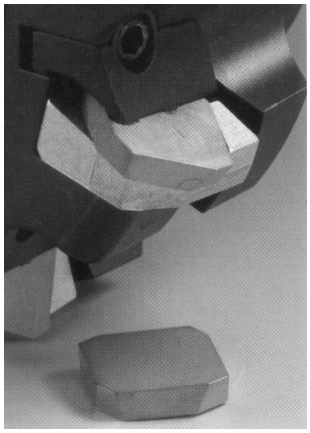

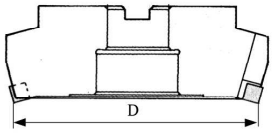


a) The R265.2-80E-20AL cutter body (D=83,6 mm)

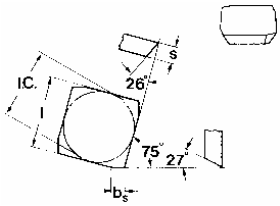


b) The SFAN 1203 EFR insert (s=3,18 mm; $b_s$=2,5 mm; l=I.C.=12,7±0,025 mm)

Fig. 2. The cutter body and the inserts

The cutting forces were monitored through a Kistler 9272 piezoelectric load cell and processed by a suitable data logging system.

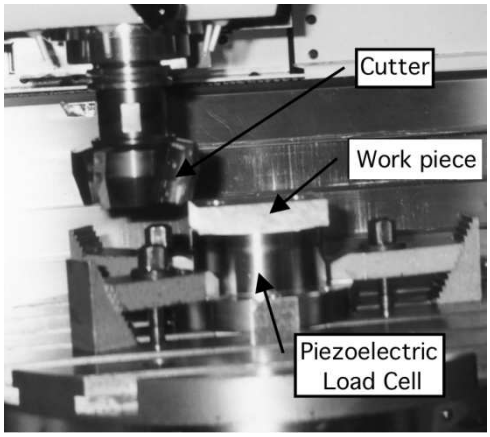


Fig. 3. Detail of the experimental outfit

As one can see in Fig. 3, the work pieces are bolted to the load cell, which in turn is bolted to the table of the machining centre. The dimensions of the paralellepiped work pieces were 96 mm x 62 mm x 20 mm and two counterbored holes were made for fastening to the load cell, as shown in Fig. 4.

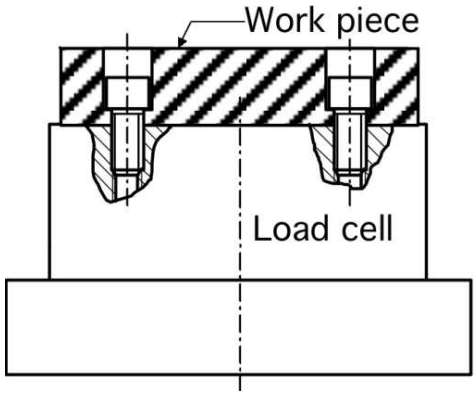


Fig. 4. Fixing the work piece

**2.1 The experimental results**

The results of the 36 runs required for carrying out the CCD plan that was implemented are included in Table 3.

Table 3. The experimental results

| Run no. | Variables | | | | Response | |
|---|---|---|---|---|---|---|
| | $v$ (m/min) | $f_z$ (mm) | HB | $a_p$ (mm) | $F_c$ (N) measured | $k_s$ (N/mm$^2$) |
| 1 | 700 | 0,10 | 98 | 0,60 | 49 | 819 |
| 2 | 947 | 0,10 | 98 | 0,60 | 51 | 848 |
| 3 | 700 | 0,20 | 98 | 0,60 | 88 | 732 |
| 4 | 947 | 0,20 | 98 | 0,60 | 82 | 685 |
| 5 | 700 | 0,10 | 148 | 0,60 | 54 | 906 |
| 6 | 947 | 0,10 | 148 | 0,60 | 54 | 906 |
| 7 | 700 | 0,20 | 148 | 0,60 | 92 | 763 |
| 8 | 947 | 0,20 | 148 | 0,60 | 95 | 794 |
| 9 | 700 | 0,10 | 98 | 2,30 | 163 | 709 |
| 10 | 947 | 0,10 | 98 | 2,30 | 168 | 732 |
| 11 | 700 | 0,20 | 98 | 2,30 | 290 | 630 |
| 12 | 947 | 0,20 | 98 | 2,30 | 286 | 622 |
| 13 | 700 | 0,10 | 148 | 2,30 | 181 | 789 |
| 14 | 947 | 0,10 | 148 | 2,30 | 180 | 782 |
| 15 | 700 | 0,20 | 148 | 2,30 | 341 | 742 |
| 16 | 947 | 0,20 | 148 | 2,30 | 323 | 703 |
| 17 | 602 | 0,14 | 120 | 1,17 | 138 | 840 |
| 18 | 1100 | 0,14 | 120 | 1,17 | 126 | 768 |
| 19 | 814 | 0,07 | 120 | 1,17 | 76 | 932 |
| 20 | 814 | 0,28 | 120 | 1,17 | 247 | 753 |
| 21 | 814 | 0,14 | 70 | 1,17 | 113 | 691 |
| 22 | 814 | 0,14 | 167 | 1,17 | 141 | 862 |
| 23 | 814 | 0,14 | 120 | 0,30 | 44 | 1039 |
| 24 | 814 | 0,14 | 120 | 4,50 | 480 | 762 |
| 25 | 814 | 0,14 | 120 | 1,17 | 139 | 851 |
| 26 | 814 | 0,14 | 120 | 1,17 | 136 | 829 |
| 27 | 814 | 0,14 | 120 | 1,17 | 139 | 851 |
| 28 | 814 | 0,14 | 120 | 1,17 | 140 | 857 |
| 29 | 814 | 0,14 | 120 | 1,17 | 132 | 807 |
| 30 | 814 | 0,14 | 120 | 1,17 | 132 | 807 |
| 31 | 814 | 0,14 | 120 | 1,17 | 138 | 840 |
| 32 | 814 | 0,14 | 120 | 1,17 | 138 | 840 |
| 33 | 814 | 0,14 | 120 | 1,17 | 136 | 829 |
| 34 | 814 | 0,14 | 120 | 1,17 | 138 | 840 |
| 35 | 814 | 0,14 | 120 | 1,17 | 136 | 829 |
| 36 | 814 | 0,14 | 120 | 1,17 | 137 | 834 |

From Fig.s 5, 6 and 7 one can conclude that it is likely that all the relevant variables were taken into account and that no bias occurs (Montgomery, 1991).

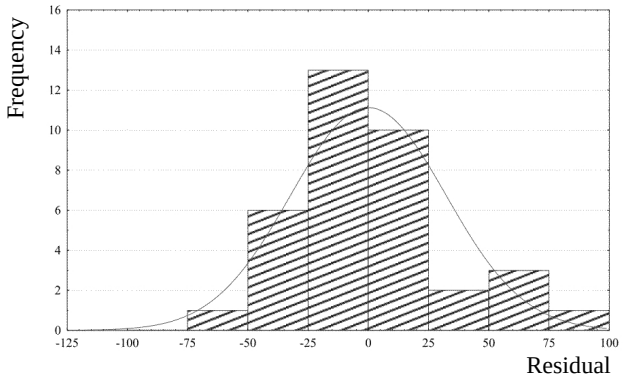


Fig. 5. Histogram of residuals

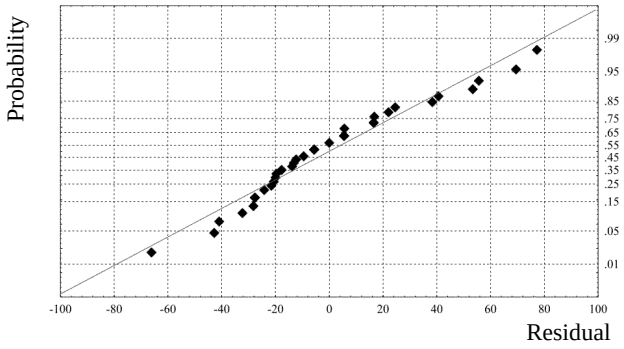


Fig 6. Normal probability plot of residuals

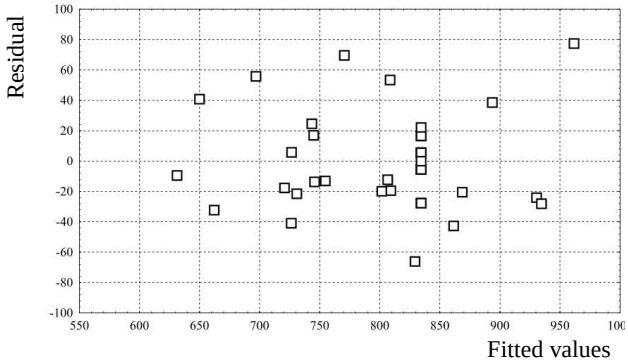


Fig. 7. Plot of residuals vs. fitted values

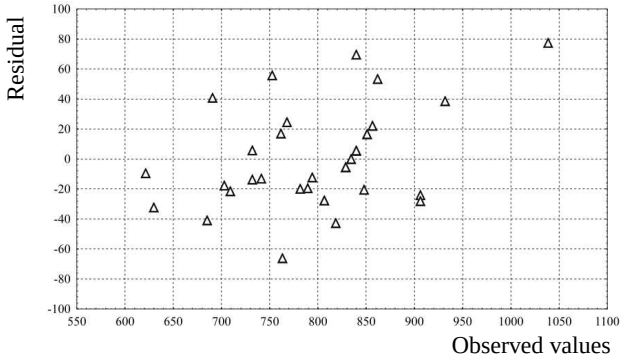


Fig. 8. Plot of residuals vs. observed values

The analysis of variance for $k_s$ can be seen in Table 4, and Table 5 shows the regression coefficients of the empirical model that we were looking for. The relevant items are shown in bold face in both tables and the corresponding second-degree polynomial function is expressed by

$$k_s = 834 - 19\ v^2 - 49\ f_z + \\ +40\ \mathrm{HB} + 26\ \mathrm{HB}^2 - 54\ a_p, \quad (7)$$

with a confidence interval of 95%.

Table 4. The ANOVA table

| $R^2$= 0,8512; $R^2_{Adjust}$= 0,752<br>Factors: 4; Blocks: 1; Runs: 36 | | | | |
|---|---|---|---|---|
| | SS | d.o.f. | MS | F |
| $v$ | 1086,7 | 1 | 1086,71 | 0,62620 |
| **$v^2$** | 12003,3 | 1 | 12003,27 | **6,91669** |
| **$f_z$** | 58047,7 | 1 | 58047,65 | **33,44900** |
| $f_z^2$ | 3070,2 | 1 | 3070,18 | 1,76914 |
| **HB** | 37739,3 | 1 | 37739,25 | **21,74662** |
| **HB$^2$** | 22092,9 | 1 | 22092,93 | **12,73069** |
| **$a_p$** | 70383,8 | 1 | 70383,83 | **40,55752** |
| $a_p^2$ | 712,4 | 1 | 712,39 | 0,41050 |
| $v\ f_z$ | 712,9 | 1 | 712,90 | 0,41080 |
| $v$ HB | 9,5 | 1 | 9,52 | 0,00549 |
| $v\ a_p$ | 127,3 | 1 | 127,33 | 0,07337 |
| $f_z$ HB | 205,4 | 1 | 205,40 | 0,11836 |
| $f_z\ a_p$ | 2198,3 | 1 | 2198,33 | 1,26675 |
| HB $a_p$ | 82,3 | 1 | 82,34 | 0,04745 |
| Err. | 36443,6 | 21 | 1735,41 | |
| SS Total | 244915,6 | 35 | | |
| $F_{(14;\ 21;\ 0,05)}$ = 2,59 | | | | |

Table 5. The regression coefficients for $k_s$

| $R^2$= 0,8512; $R^2_{Adjust}$= 0,752<br>Factors: 4; Blocks: 1; Runs: 36 | | | |
|---|---|---|---|
| | Coeficient | Std. Err. | t (21) |
| **Constant** | **834,485** | 12,02569 | **69,39181** |
| $v$ | -6,729 | 8,50345 | -0,79133 |
| **$v^2$** | **-19,368** | 7,36420 | **-2,62996** |
| **$f_z$** | **-49,180** | 8,50345 | **-5,78351** |
| $f_z^2$ | -9,795 | 7,36420 | -1,33009 |
| **HB** | **39,654** | 8,50345 | **4,66333** |
| **HB$^2$** | **-26,276** | 7,36420 | **-3,56801** |
| **$a_p$** | **-54,154** | 8,50345 | **-6,36848** |
| $a_p^2$ | 4,718 | 7,36420 | 0,64071 |
| $v\ f_z$ | -6,675 | 10,41456 | -0,64093 |
| $v$ HB | -0,772 | 10,41456 | -0,07408 |
| $v\ a_p$ | -2,821 | 10,41456 | -0,27088 |
| $f_z$ HB | 3,583 | 10,41456 | 0,34403 |
| $f_z\ a_p$ | 11,722 | 10,41456 | 1,12550 |
| HB $a_p$ | 2,269 | 10,41456 | 0,21783 |
| $t_{(21;\ 0,05)}$ = 2,080 | | | |

The values of $F_c$ in Table 3 were obtained through the tests carried out with the described experimental outfit and were used to compute $k_s$ through Eq. (2).
The Kistler 9272 load cell was used to measure three orthogonal components of the cutting force along the spindle direction (z), the feed direction (x), and the normal direction (y), as shown in Fig. 9. Noting that the component $F_Z$ can be neglected due to the specific geometry of the tool, it follows that the cutting force belongs to the plane xy and is the vectorial sum of $F_x$ and $F_y$, wich is denoted by $F_{Res}$ in Fig. 9.

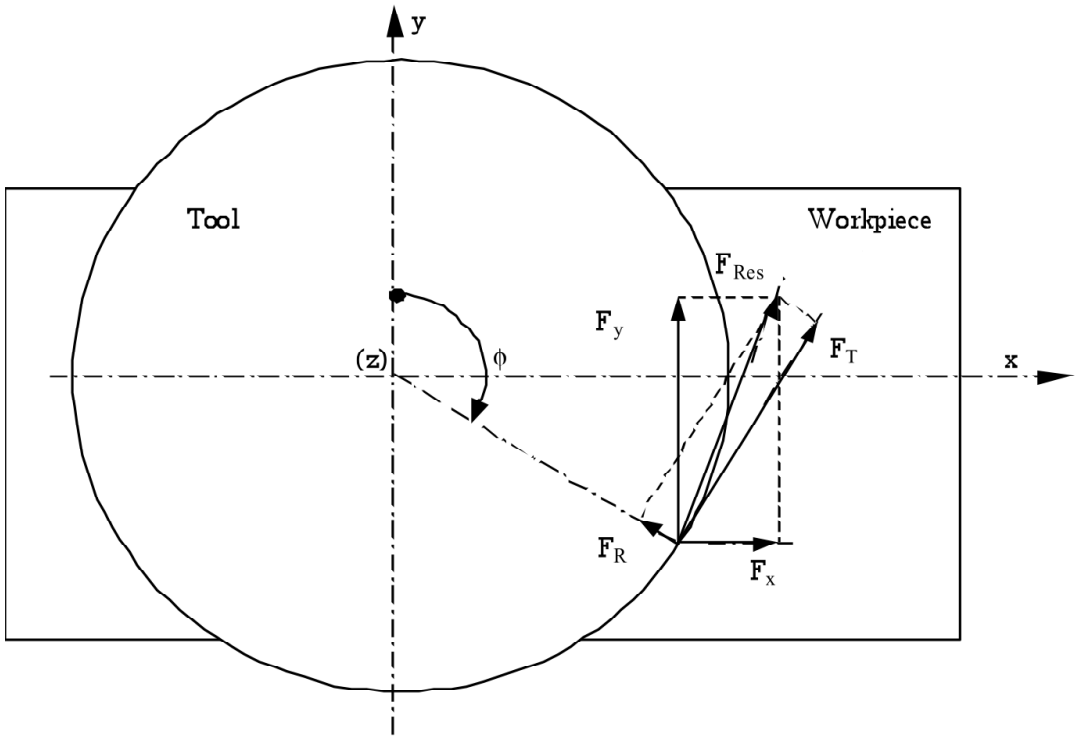


Fig. 9. The forces exerted over the tool

Fig. 9 also allows for concluding that we have $F_y = F_T$ and $F_x = F_R$ for $\phi = \pi/2$. In our case, the sampling rate of the data loging system was sufficiently high to acquire $F_x$ and $F_y$ at $\phi = \pi/2$ with a maximum error that ranges from 2,75º (for the lowest rotational speed of the spindle that was used in our experiments) to 5,0º (for the highest rotational speed).

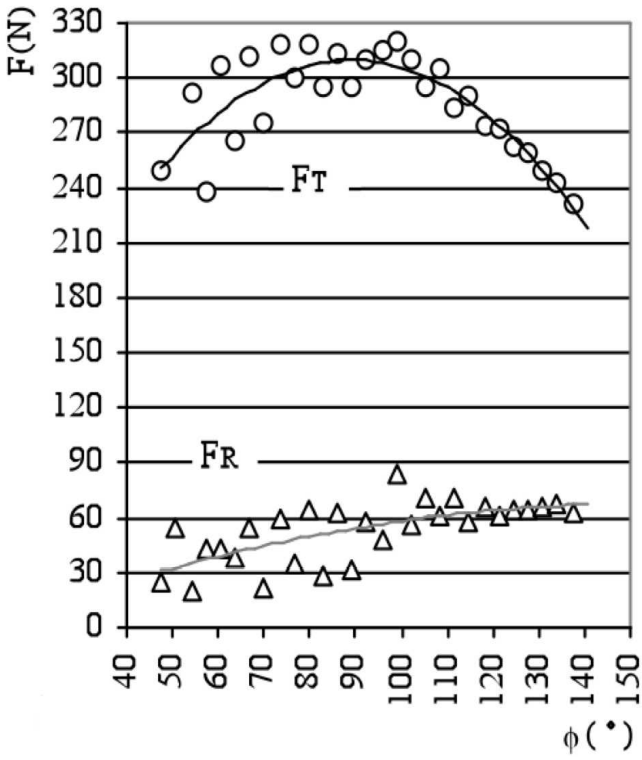


Fig. 10. Mean values of $F_T$ and $F_R$ for eight consecutive circular passes of the cutting edge (Mourão 1999)

As one can see in Fig. 10, the tangencial component of the cutting force at $\phi = \pi/2$ is more than five times higher that the radial one. For our experiments, in addition, the tangential speed of the tool was tipically $10^3$ times higher than the feed speed, which means that the contribution of the radial force for the specific cutting energy can be neglected.
In other words, one can say that the tangencial force $F_T$ is a good approximation of the cutting force $F_c$ in Eq. (2) and in Table 3. This simplification was adopted in the present work.

## 3. DISCUSSION

As it was shown, there are some factors that considerably affect the specific cutting energy in face milling of aluminium alloys with wiper edge inserts. In fact, from Eq. (7) one can see that:

1) The specific cutting energy decreases with the increasing of the squared cutting speed of the mill, which means that the sensivity to this variation increases with the cutting speed.
2) The specific cutting energy decreases with the increase of both the feed per tooth, $f_z$, and the depth of cut, $a_p$.
3) The influence of the variation of the depth of cut in the specific cutting energy is marginally stronger than the variation of the feed per tooth.
4) The higher is the hardness of the work piece the higher is the specific cutting energy, and the sensivity to the variation of the hardness is higher for higher hardness values.

## 4. CONCLUSIONS

The accurate estimation of the cutting forces in milling operations is important for planning and setting up high productivity machining processes. However, the aforesaid estimation critically depends on the prediction of the specific cutting energy, which in turn depends on the hardness of the material to be machined, on the cutting parameters, and on the geometry of the tool and inserts.

In spite of this, the traditional formulae used to compute the specific cutting energy just take into account either the feed per tooth or the thickness of the unformed chip. Yet, the variety of the insert shapes that are being used nowadays should also be considered.

Beside to finishing operations, wiper edge inserts are used more and more for rough cutting with increasing productivity without compromising the final surface quality. Some manufacturers also claim that wiper edge technology prevents the occurrence of chatter to some extent.

This paper concerns to the specific cutting energy in face milling of aluminium alloys with zero nose radius wiper edge inserts.

The coefficients of Eq. (7) result from the experiments presented in this paper and show that the specific cutting energy for this case is similarly influenced by the depth of cut and by the feed per tooth. The results also show that the cutting speed should not be neglected, and that the influence of the depth of cut, $a_p$, for the magnitude of the cutting force (and therefore for the magnitude of the specific cutting energy) is lesser than the one that is predicted by Eq. (1), in which the consequences of changing the cutting speed are neglected. Nevertheless, one should notice that Eq. (7) shows that the specific energy decreases with the increase of the squared cutting speed.

Incidentally, the maximum cutting speed that was possible to use in our experiments was 1 100 m/min due to the maximum value of the spindle rotational speed of the machine centre and to the diameter of the cutter that were used. Even so, it is worth to remark that the inserts that were used in the experiments would easily allow much higher cutting speeds. Hence, it would be very interesting to explore experimentally the influence of even higher cutting speeds in the specific cutting energy, since the results of this kind of studies are not common and would make easier the planning of high speed milling operations.

Additionally, the peripheral speeds of the tool that were used in the face milling of aluminium alloys of our study are much higher that the feed speed. Therefore, the tangencial component of the cutting force was more than five times higher that the radial one. In our experiments, the tangential speed of the tool was tipically $10^3$ times higher than the feed speed, which means that the contribution of the radial force for the specific cutting energy can be neglected. In other words, one can say that the tangencial force is a good approximation of the cutting force. This allowed us for using the tangencial force instead of the cutting force without significant lack of accuracy.

Therefore, in spite of the limited cutting speed range that was used in our study, one can conclude that zero-nose radius wiper edge inserts allow improving the productivity of face milling operations in aluminium alloys. In fact, Eq. (7) shows that the higher are the values of the cutting speed, of the feed per tooth and of the depth of cut, the lower is the specific cutting energy.

At last, taking into account the current variety of cutting tool geometries, it is likely that there will be good prospects for developing research work in the area of specific cutting energy, as a means to attain the maximum productivity of machining operations for different tool geometries.

## 5. REFERENCES

1. Jain, V.K., Bandyopadhyay, D.K. (1986). *Shear Angle During Accelerated Cutting: Response Surface Approach*, Int. J. of Machine Tools and Manufacture, Vol. 26, No. 1, pp. 35-50.

2. Kennametal, *Techical Tip 131 – Beneficts of Using Wiper Inserts in Turning Applications*. Available from: www.kennametal.com/images/pdf/customer_support/tech_tips/TechTip_131_WiperInsertBenefits_Turning.pdf, Acessed: 25/01/2010.

3. Khabeery M.E. El-, Fattouh M. (1986), *Residual Stress Distribution Caused by Milling*, Int. J. of Machine Tools and Manufacturing Vol. 29, No. 3, pp. 391-401.

4. Mitsubishi, *Wiper Insert*. Available from: http://www.mitsubishicarbide.net/mmus/en/product/product_guide/information/turning/wipertip.html, Accessed: 25/01/2010.

3. Montgomery, D.C. (1991). *Design and Analysis of Experiments*, 3rd Ed., John Wiley & Sons, N.Y.

4. Mourão A. (1999). *A Influência dos Parâmetros de Fresagem na Rugosidade de Superfícies Facejadas em Ligas de Alumínio*. Ph.D. Thesis, Universidade Nova de Lisboa, Campus de Caparica.

5. Rodrigues, A.R., Coelho, R.T. (2007). *Influence of the Tool Edge Geometry on Specific Cutting Energy at High-Speed Cutting*, J. of the Braz. Soc. of Mech. Sci. & Eng., Vol. XXIX, No. 3, pp. 279-283.

6. Sandvik-Coromant (1994), *Modern Metal Cutting - A practical Handbook*, Sandvik-Coromant Technical Editorial Department, Sandviken, Sweden.

Received: June 21, 2010 / Accepted: November 20, 2010 / Abstract published online: December 5, 2010
© International Journal of Modern Manufacturing Technologies